Supporting Information

Nature-inspired functional porous materials for low-concentration biomarkers detection

Irene Papiano[‡], Simona De Zio[‡], André Hofer, Marco Malferrari, Ignacio Mínguez Bacho, Julien Bachmann, Stefania Rapino, Nicolas Vogel, Giulia Magnabosco*

Irene Papiano, Nicolas Vogel, Giulia Magnabosco: Institute of Particle Technology (LFG), Friedrich-Alexander-University Erlangen-Nürnberg (FAU), Cauerstraße 4, 91058 Erlangen, Germany. Giulia Magnabosco: giulia.magnabosco@fau.de

Irene Papiano, Simona De Zio, Marco Malferrari, Stefania Rapino: Department of Chemistry "Giacomo Ciamician", University of Bologna, Via Selmi 2, 40126 Bologna, Italy

André Hofer, Ignacio Mínguez Bacho, Julien Bachmann: Chair 'Chemistry of Thin Film Materials' (CTFM), Friedrich-Alexander University Erlangen-Nürnberg (FAU), IZNF, Cauerstraße 3, 91058 Erlangen, Germany

Further morphological characterization

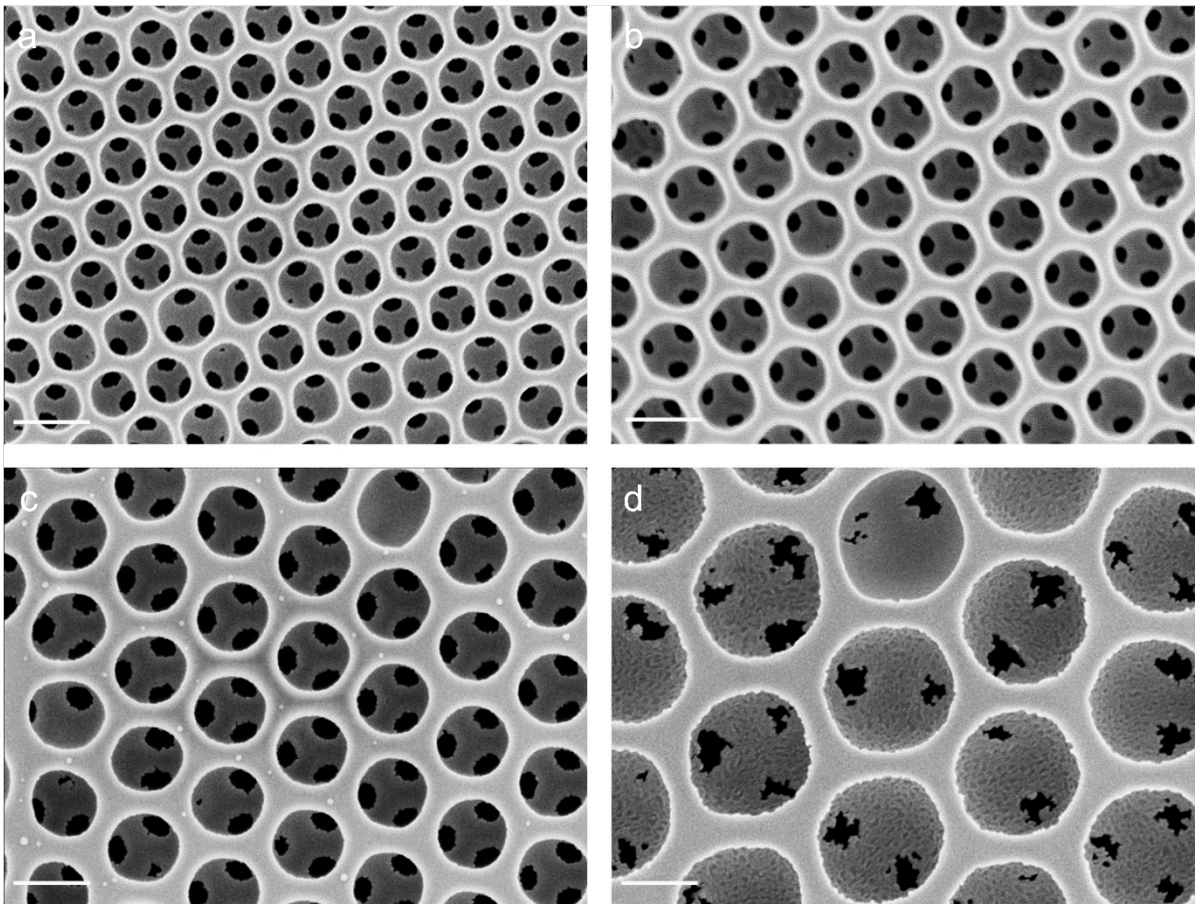

Figure S1. SEM images of IOs produced with (a) 220 nm, (b) 290 nm, (c) 350 nm, (d) 565 nm diameter colloids. Scalebar is 300 nm.

EDS quantification of Pt and Zn

	Si – K series	Zn – L series	Pt – M series
Weight %	13.29	38.29	23.28
Weight % error	± 0.14	± 0.27	± 0.55
Atom %	17.04	21.39	4.30
Atom % error	± 0.18	± 0.15	± 0.10

Table S1. Qualitative elemental analysis of IOs coated with 4 nm AZO and 1 nm Pt using the SEM-EDX technique.

Electrochemical characterization

Optimization of AZO thickness

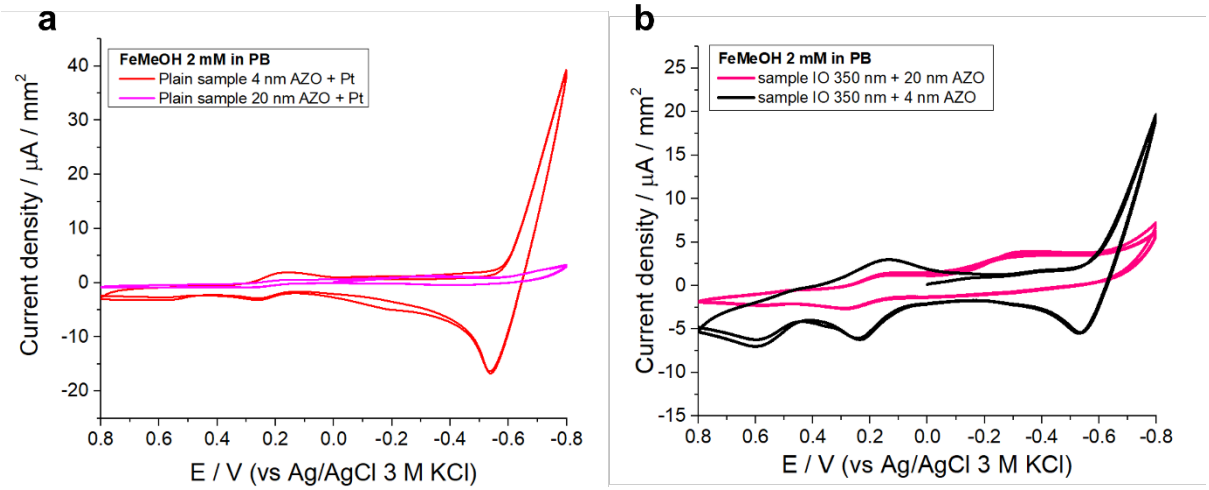

Figure S2. Cyclic voltammograms of plain samples (a) and IO (b) covered with 4 or 20 nm AZO. The CVs are registered in a solution of 2 mM FeMeOH in PB. Potential scan from -0.8 to 0.8 V vs. Ag/AgCl (3 M KCl), scan rate 20 mV/s.

Cyclic voltammetries were conducted on IOs covered with 4 or 20 nm AZO (Figure SI2b) to investigate the ideal AZO thickness. The electric current resulted to be higher for the opals coated with 4 nm AZO rather than 20 nm. The same trend is also present in the plain samples coated with the same amount of metallic materials chosen as reference system (Figure SI2a).

Cyclic voltammetry-Figure 2f extended discussion

Figure 2f reports cyclic voltammetry of IOs with 4 nm (black) and 20 nm (blue) AZO. Here we describe the peak assignation.

According to the Randles-Sevcik equation (Equation SI1) that describes the linear dependence of the peak current on the surface area, we can confirm the enhancement of the accessible surface area provided by the interconnected porous network of the inverse opal. We demonstrate that the chemical species have access not only to the outer surface of the IO, but also to the inner structure. Moreover, the AZO deposited on the surface does not limit the diffusion of the redox species toward the pores. Therefore, the IO-based electrodes provide an optimal permeation of chemical species within the porous structure with the subsequent possibility to immobilize them on a large surface area, having significant effects on the biosensors' sensitivity (e.g. immobilization of the enzyme).

$$i_p = 0.446nFAC^0\sqrt{\frac{nFvD_0}{RT}}$$

Equation S1. Randles-Sevcik equation, where i_p (A) is the peak current, n the number of electrons transferred in the redox process, F the Faraday constant, A (cm^2) the electrode surface area, C^0 (mol/cm3) the bulk concentration of the redox species, v (V/s) the scan rate, D_0 (cm^2/s) the diffusion coefficient of the redox species.

Several electrochemically processes take place in the potential window of the performed cyclic voltammograms in water solution and in the presence of redox species, i.e. ferrocene methanol (2 mM in PB) and oxygen. FcMeOH is a neutral redox species, and its reversible electrochemical oxidation reaction was chosen to study the electron transfer characteristics of the IO-based electrode. Both the voltammograms in figure 2f show the water reduction at – 0.8 V vs. Ag/AgCl and the redox peaks of ferrocene methanol at 0.14 V vs. Ag/AgCl (reduction) and at 0.24 V vs. Ag/AgCl (oxidation), in agreement with the reported standard potentials of this specie[1]. The experimental half-wave potential is $E_{1/2}$ = 201 mV vs Ag/AgCl (3 M KCl) and ΔE_p = 117 mV, which reports for a not zero resistance of the system. From the aforementioned discussed results, we can conclude that the metal-coated porous substrate is a good electrodic material. In addition, the voltammogram lacks adsorption/desorption peaks indicating high stability of the inverse opal-based structures in the explored potential window.

To properly attribute the redox peaks, we also registered the voltammograms of FcMeOH using ITO and Pt as electrodic materials of the working electrodes (Figure SI3a,b).

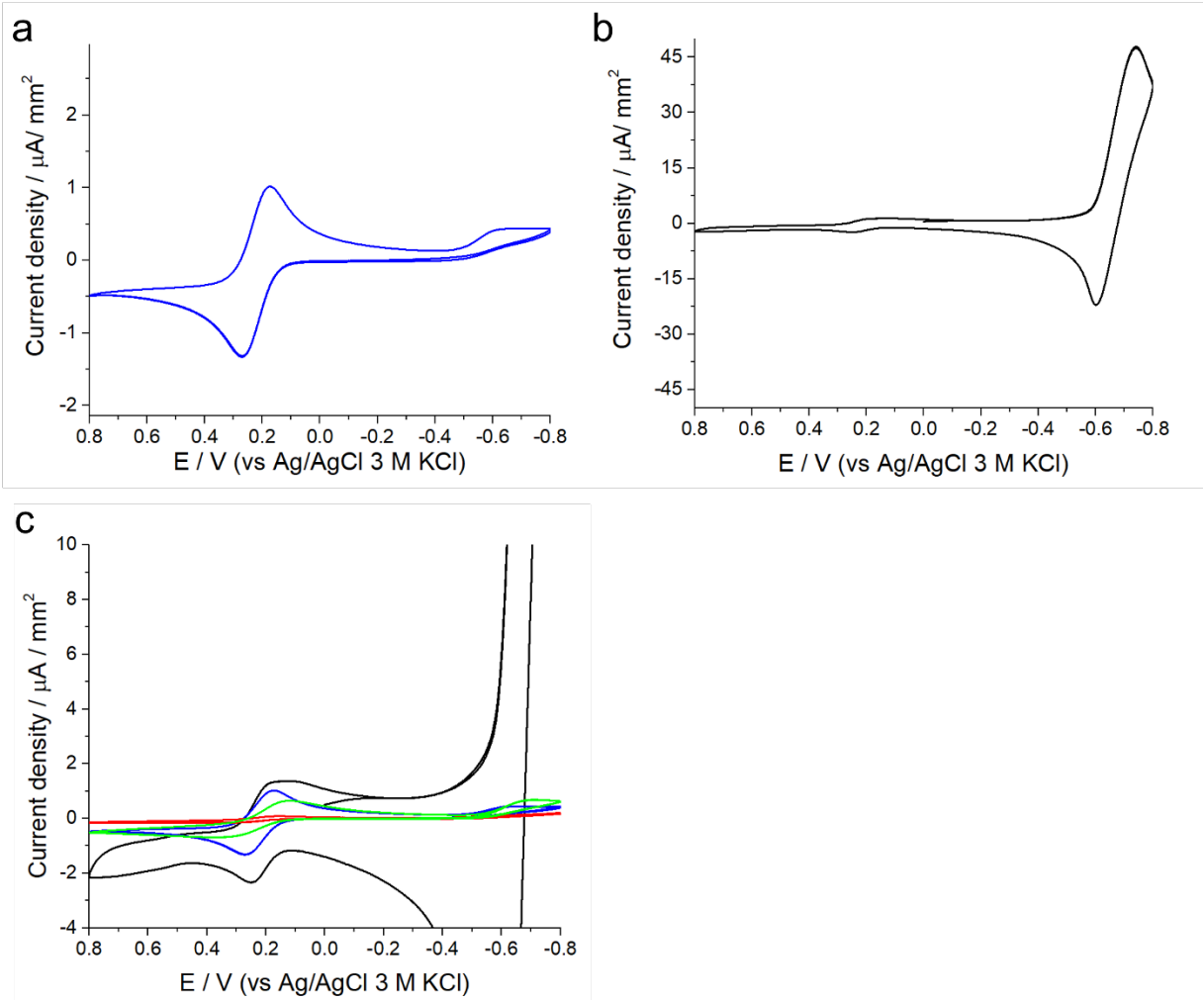

Figure S3. Cyclic voltammograms of ITO-coated glass slide (a), Pt (b), and overlay of the voltammograms of the isolated components and final electrode (c- ITO-coated glass slide (blue), Pt (black), ITO glass slide covered with AZO (red) and IO covered with AZO (green)). The CVs are registered in a solution of 2 mM FcMeOH in PB. Potential scan from - 0.8 to 0.8 V vs. Ag/AgCl (3 M KCl), scan rate 20 mV/s.

In the voltammogram of Pt (Figure SI3b) we can appreciate the typical H_2 adsorption peak at – 0.755 V vs. Ag/AgCl and the H_2 desorption peak at -0.600 V vs. Ag/AgCl, both characterized by very high current values[2]. Platinum oxide formation occurs at 0.680 V vs. Ag/AgCl, and its reduction peak is at 0.086 V vs. Ag/AgCl, in agreement with the literature[2]. However, the Pt peaks are not clearly visible either in the nanostructured and in the plain electrode (figure SI3c). FcMeOH peaks are still present both in the CVs reported in the Figure SI3a and in Figure SI3b. In the ITO voltammogram in Figure SI3a we can also notice a reduction peak at – 0.614 V vs. Ag/AgCl that can be attributed to the reduction of SnO_2[3]. The latter redox peak is not visible in the voltammograms conducted on the nanostructured and plain samples (Figure SI3c). By comparing the votammogram of a plain AZO sample and the IO AZO-coated sample (figure SI3c) we ascribe the peaks observed at -0.439 V vs. Ag/AgCl (reduction) and at 0.570 V vs. Ag/AgCl (oxidation) to the presence of AZO on the substrate.

Electrochemical setups used for electropolymerization and electrochemical measurements

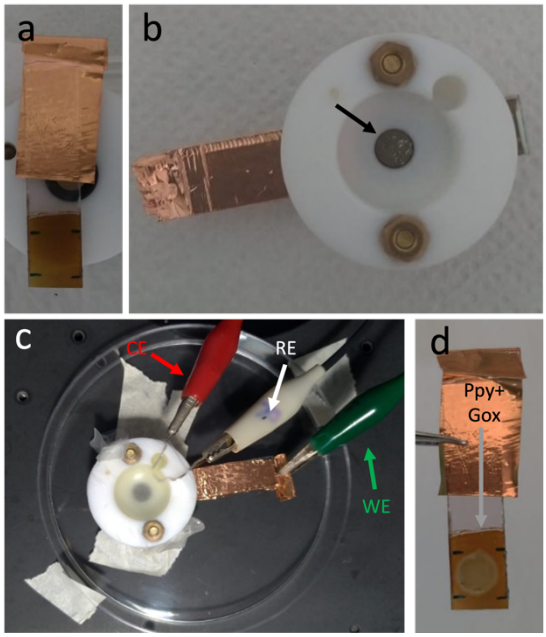

Figure S4. Step-by-step electropolymerization procedure and experimental setup. (a) Pt-AZO-covered IO on ITO substrate with copper tape contact. (b) IO-based electrode inside the electropolymerization cell. The area in which the electropolymerization will take place is highlighted with an arrow. (c) Electrochemical setup for electropolymerization. The Ppy+Gox solution is added to the cell, and the counter electrode (CE) and reference electrode (RE) are immersed in the solution. The copper tape connected to the IO is used to set up the connection of the working electrode (WE). The same configuration was used for the electrochemical measurements. (d) Final sensor. The arrow highlights the area where the Ppy+Gox were deposited. The change in color is due to the filling of the pores.

Estimation of the quantity of GOx immobilized on the IO-based biosensor

The quantity of GOx immobilized on the sensor has been estimated via an independent electrochemical method, that is the determination of the glucose concentration in 1 mL of PBS before and after its exposition to the GOx, immobilized on a sensing platform. The glucose concentration was reduced from 1 mM (initial concentration) to 0.79 mM (final

concentration) due to its oxidation by the enzyme immobilized on the platform during 2h of immersion.

On this base, using a range of tabulated values for the turnover number for GOx from Aspergillus Niger at pH 7.4,[4] we estimate that $5.2*10^{10}$ - $5.9*10^{13}$ enzyme molecules are present on the surface we analyzed. We can convert it in mass of enzyme per planar surface area ($7*10^{-4}$ µg/ mm^2 - $7.9*10^{-1}$ µg/ mm^2) or unit of enzymes per planar surface area ($1.14*10^{-4}$U/ mm^2 – $1.3*10^{-1}$ U/mm^2).

Current response of IO/AZO/Pt substrate to H_2O_2 administration.

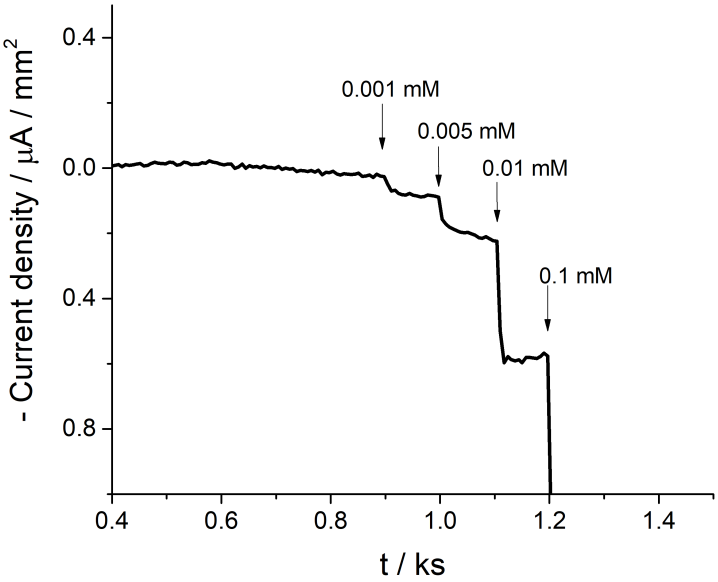

Figure S5. Chronoamperometic measurements of Pt-covered-AZO/IO. The arrows correspond to H_2O_2 additions in the solution. The curves are registered in PBS solution at RT, *E* = + 0.65 V vs Ag/AgCl (3 M KCl).

Current response of IO-based biosensor to glucose administration.

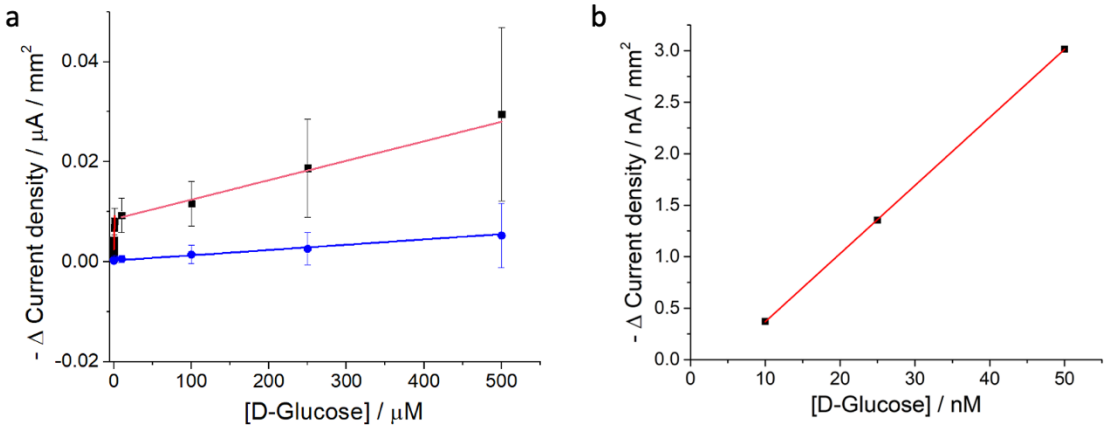

Figure S6. Change in current density of the glucose biosensors based on Pt-covered-AZO/IO and plain counterpart used for the calculation of the LOD. The curves are registered in PBS solution at RT, *E* = + 0.65 V vs Ag/AgCl (3 M KCl). (a) Change in current density of Pt-covered-AZO/IO (black squares) and electrode with no nanostructuration (blue points) with additions of glucose reported in linear scale. The calculated slopes are: $6.9*10^{-3}$ µA/µM for the first glucose concentration range (0.01-1 µM) of the IO-based biosensor (red), $3.9*10^{-5}$ µA/µM for the second glucose concentration range (10-500 µM) of the IO-based biosensor (pink), $1.06*10^{-5}$ µA/µM for the plain biosensor (blue). Bars represent standard deviations of the

measurements. (b) Representative behavior of the IO-based biosensor at low additions of glucose. The LOD obtained from the linear regression of the response to glucose additions 10, 25 e 50 nM is 0.4 nM.

Stability test over 72 hours

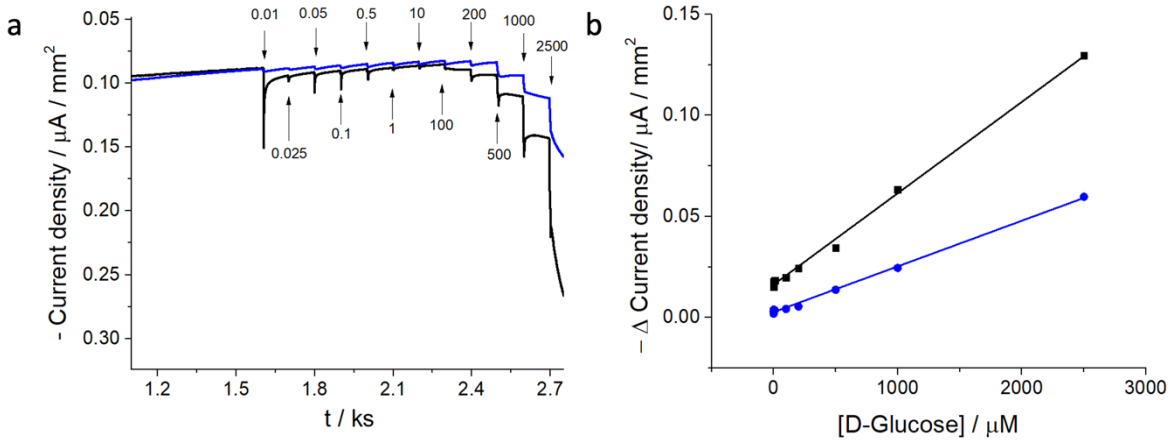

Figure S7. Evaluation of the stability of the sensor. (a) Chronoamperometric measurements of standard additions for freshly prepared (black) and stressed IO-based biosensor stored in PBS and tested after 72 h (blue). The curves are registered in PBS solution at RT, E = + 0.65 V vs Ag/AgCl (3 M KCl). The additions indicated by the arrows are expressed in µM. (b) Change in current density at t=0 (black) and at t=72h (blue) upon standard additions of glucose. The slopes are respectively $4.52*10^{-5}$ µA/ µM for the biosensor at first use and $2.26*10^{-5}$ µA/ µM for the biosensor after 72h. 50% of the activity is retained after 72h.

We investigated the performances of our sensor over an extended period of time and with high glucose concentration, much higher than the envisioned working range, to assess its behavior under conditions of extreme stress. After a 72-hour period and under high stressing working conditions (Figure SI7), the sensor is still able to detect changes in current density. Given that the conditions used for the test really push the boundary of the sensor far out from the envisioned condition applications (i.e. use in body fluid with lower concentrations of glucose than blood, e.g. tears or saliva), we considered the retained sensitivity as the lowest limit of sensitivity under stress.

References

[1] C. L. Lin, J. Rodríguez-López, A. J. Bard, *Analytical Chemistry* **2009**, *81*, 8868.
[2] G. Denuault, *Ocean Science* **2009**, *5*, 697.
[3] P. Vanýsek, *The Encyclopedia of Chemical Electrode Potentials* **1982**, 20.
[4] I. Schomburg, A. Chang, D. Schomburg, *Nucleic Acids Research* **2002**, *30*, 47.